JOURNAL OF AIRCRAFT
Vol. 39, No. 2, March–April 2002

Forebody Flow Control at Conditions of Naturally Occurring Separation Asymmetry

Lars E. Ericsson*
Mountain View, California 94040
and
Martin E. Beyers†
Institute for Aerospace Research, Ottawa, Ontario K1A 0R6, Canada

Extensive efforts have been directed toward the development of the means by which the flow separation asymmetry occurring on an axisymmetric slender forebody at very high angles of attack could be controlled in order to improve the agility of advanced aircraft and missiles. To control the asymmetric flow separation represents a great challenge, and only a few of the investigated flow-control concepts have led to viable solutions. The fluid-mechanical processes associated with steady and alternating-pulsed blowing applications are analyzed in an effort to define flow mechanisms that can cause the observed anomalous control characteristics.

Nomenclature

b^*	=	wing span or maximumm body diameter
$C_{\dot{m}}$	=	dimensionless mass flow rate of jet blowing
C_μ	=	dimensionless flow-momentum-rate of jet blowing
D	=	maximum body diameter
L	=	microrod extension (Fig. 4)
l	=	body length
ℓ	=	x location for $L = 0$ (Fig. 4)
M	=	Mach number
N	=	normal force, coefficient $C_N = N/(\rho_\infty U_\infty^2)S^*$; $c_n = \partial C_N/\partial\xi$
n	=	yawing moment, coefficient $C_n = n/(\rho_\infty U_\infty^2/2)S^*b^*$
Re	=	Reynolds number based on D and U_∞
r	=	local body radius
r_B	=	base radius
r_N	=	nose radius
S^*	=	reference area, projected wing area or $\pi D^2/4$
T	=	period of alternating blowing cycle
t	=	time
t_c	=	convection time, $= l/U_\infty$
t^*	=	dimensionless time, $t^* = x\tan\alpha/r$ (Fig. 17)
U_∞	=	freestream velocity
x	=	axial body-fixed distance from the nose tip
Y	=	side force, coefficient $C_Y = Y/(\rho_\infty U_\infty^2)S^*$; $c_y = \partial C_Y/\partial\xi$
α	=	angle of attack
Δ	=	increment
θ_A	=	apex half angle of slender forebody
ξ	=	dimensionless x coordinate, $= x/D$
ρ_∞	=	freestream fluid density
τ	=	time duration that the valve is open during the blowing cycle
ϕ	=	azimuth of blowing orifice, $\phi > 0$ on the startboard side

Received 31 July 2000; revision received 9 August 2000; accepted for publication 29 November 2001.

*Engineering Consultant. Fellow AIAA.
†Principal Research Officer, Aerodynamics Laboratory. Senior Member AIAA.

Introduction

PREVIOUS studies of fighter aircraft configurations have revealed that forebody flow-control devices can generate yaw authority that at high angles of attack, $\alpha > 30$ deg, significantly exceeds that of a conventional rudder.[1] As measurements of typical combat aircraft models have shown that the high-alpha lateral characteristics are generated by the fuselage, for example, as shown in Ref. 2, forebody-flow-control studies have largely been conducted on slender-nosed bodies of revolution.[3] The challenge presented to the designer is to find reliable means for control of the asymmetric flow separation occurring naturally on a slender forebody when the angle of attack exceeds the included apex angle, $\alpha > 2\theta_A$ (Ref. 4). A recent publication[5] gives an insightful assessment of our present understanding of the fluid-mechanical challenges associated with successful control of forebody flow asymmetry, as revealed by analysis of published results from careful computations and experiments. Closed-loop control systems have been used with success in this flow range.[5] However, that topic is beyond the scope of this paper. In the following we confine our attention to flow domains where the aerodynamic response to variations in any of the relevant parameters (angle of attack, roll angle, blowing rate, etc.) remains single valued.

Forebody Flow Control

Nose blowing has been used for control of the forebody flow asymmetry. Since it has been shown that the laminar short separation bubble plays a role in the flow separation process[6] (Fig. 1), the blowing method used by Wallis to affect the boundary layer on a stalling airfoil[7] could also be effective on bodies of revolution at high angles of attack. This is demonstrated by the results[8] in Fig. 2. Symmetric downstream blowing in the crossflow on the windward side, 30 deg below the lateral meridian (that is, between the flow stagnation and separation points) did reduce the yawing moment substantially on a cone-cylinder body; and, as in Wallis's case,[7] only minute blowing rates were needed. However, increasing the rate by two orders of magnitude, from $C_\mu = 0.00005$ to 0.00312, had no significant effect. The symmetric windward-side blowing eliminated the laminar separation bubble and changed the crossflow separation to the supercritical type, as has been verified by oil-flow studies,[8] thereby greatly reducing the crossflow asymmetry[4] occurring at $\alpha > 40$ deg $> 2\theta_A$ (Ref. 4) but not eliminating it. The results in Fig. 2 illustrate the staying power of the asymmetric forebody flow separation.

A corollary to the problem of eliminating the crossflow asymmetry occurring at $\alpha > 2\theta_A$ is the difficulty of controlling it. At the angles of attack ($\alpha > 2\theta_A$) encountered in aircraft combat maneuvers, geometric microasymmetry effects on a pointed nose control

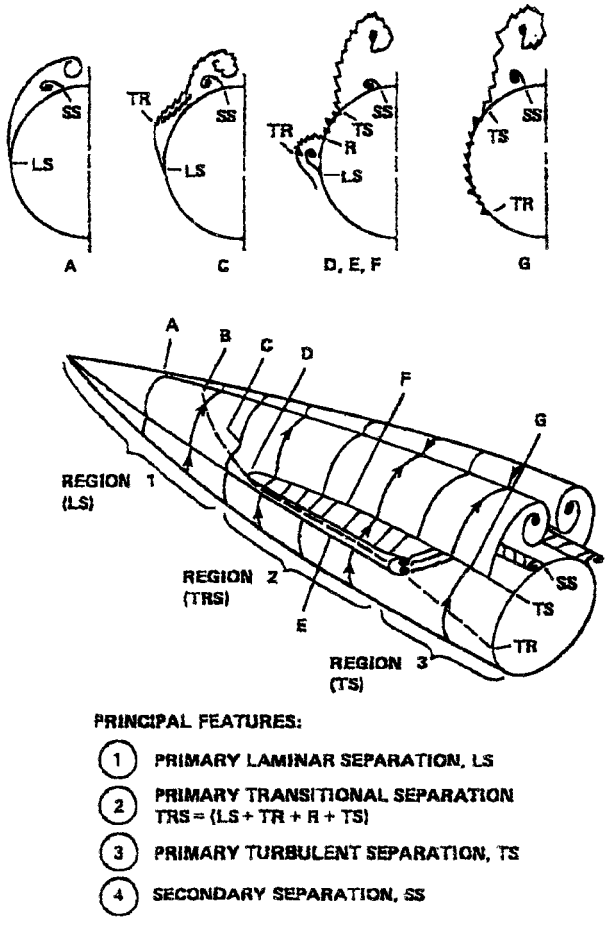

Fig. 1 Flow pattern on a 3.5-caliber pointed ogive at transitional Reynolds numbers[6] ($M = 0.55, Re = 0.8 \times 10^6, \alpha = 40$ deg, $C_Y = 0.5$).

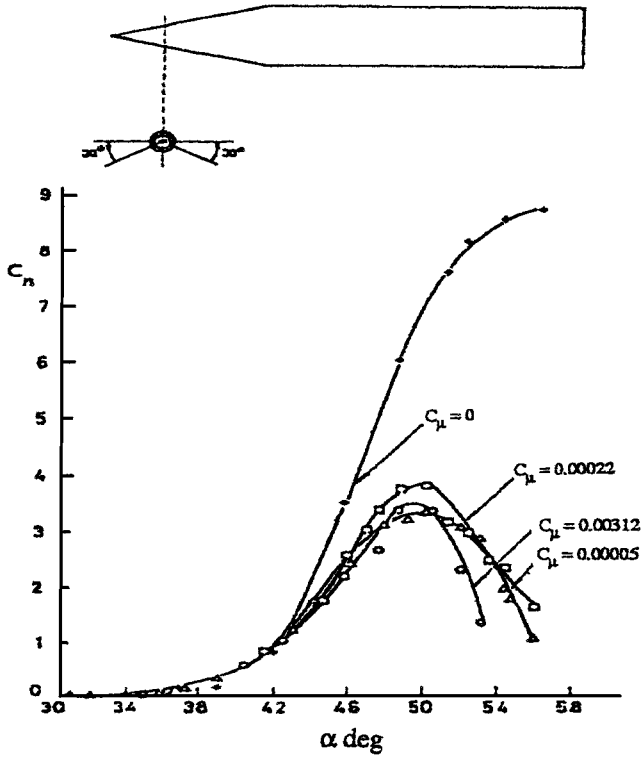

Fig. 2 Effect of symmetric windward-side nose blowing on the yawing moment induced by asymmetric crossflow separation on a cone cylinder.[8]

the direction of generated nonzero side forces and yawing moments of significant magnitude.[3,4] Because of the nature of the separation asymmetry at $\alpha > 2\theta_A$, it is relatively easy to control the direction of the generated side force at high angles of attack but very difficult to control its magnitude, as has been demonstrated by the effect of microblowing.[9] Starboard-side forward blowing at $\xi = 0.20$ and $\phi = 135$ deg on the nose of a smooth, pointed 3.5-caliber tangent-ogive was used to promote crossflow separation, giving the results shown in Fig. 3. The blowing had to be increased substantially ($C_{\dot{m}} \to 0.00020$) before the effect of the initial geometric microasymmetry, dominant at $C_{\dot{m}} = 0$, could be overpowered, causing the constant-magnitude side force to change direction. (Note the unusual definition of positive side force,[9] used here as well as in Figs. 6 and 7 to be discussed later shown in Figs. 3, 4, and 5). At $\alpha \geq 50\,\text{deg} > 2\theta_A = 32.5$ deg, asymmetric flow separation and body vortices will always be present,[4] remaining steady until $\alpha > 60$ deg, when Karman vortex shedding starts occurring on the aftbody.[10,11] The fact that the magnitude $|C_Y|$ in Fig. 3 essentially remained unchanged indicates that the starboard blowing acted only to overpower the dominant port-side microasymmetry effect present at $C_{\dot{m}} = 0$, flipping the separation asymmetry and associated side force in the opposite direction when $C_{\dot{m}} \to 0.00020$.

As the forward blowing was designed to promote crossflow separation[9] (Fig. 3), it is at first surprising that $C_{\dot{m}} \to 0.00020$ was required for the blowing to have any effect. That indicated that the effect of nose blowing was more complicated than what was originally envisioned. Experimental results for a pointed 3.5-caliber tangent-ogive-cylinder[12] (Fig. 4) illustrate the physical flow process generating the highly nonlinear, almost discontinuous C_Y characteristics in Fig. 3, where the forward blowing in many respects could have acted as the wire-protrusion in Fig. 4, both promoting asymmetric crossflow separation when acting well aft of the nose tip. (The authors are thankful to the reviewer that alerted us to the existence of Ref. 12.) At $\alpha = 40$ deg in Fig. 4, $\alpha/\theta_A = 2.44 > 2$, and only asymmetric crossflow separation exists,[4] the direction of which is determined by the combined effects of existing microasymmetries and the perturbation mechanism. When the wire approaches the nose tip ($L/D \leq 1/D = 0.095$), the side force flips to the opposite direction, both for $\phi = 45$ and 170 deg. As the body had been rotated 125 deg to move the wire-rod mechanism between the starboard side locations at 45- and 170-deg azimuth, the aggregate effect of the body microasymmetries had also been rotated 125 deg, explaining the opposite directions of the side force at $L/D = 0$ for $\phi = 45$ and 170 deg. The windward location $\phi = 45$ deg of the fully retracted rod mechanism at $L/D = 0$ could have generated a disturbance that promoted crossflow separation, thereby contributing to the negative side force. In contrast, rotating the tangent-ogive 125 deg leaves the opening window of the microrod in the aft leeward location, where it could have little effect by itself. That is, the result is similar to that obtained by rotating the nose tip of a pointed tangent-ogive[13] (Fig. 5). When the wire rod was extended on the leeward side to $L/D \approx 0.05$, its disturbance could apparently overpower the effect of body microasymmetries to switch the side force into the opposite, port-side direction (Fig. 4).

The results indicate that in both cases, for $\phi = 45$ deg as well as for $\phi = 170$ deg, when the wire rod approaches the body nose tip ($L/D \to \ell/D$ in Fig. 4) it no longer acts as a microasymmetry but rather as a local distortion of the axisymmetric geometric shape, generating an asymmetric nose bluntness effect. This would practically eliminate the side force generated on that side according to measurements for the 20% bluntness of the present tangent-ogive[14] (Fig. 6). The nose bluntness removes the geometric singularity generated by the pointed nose, which according to experimental results[15] for a paraboloid nose shape (Fig. 8) would greatly limit its capability to generate any significant side force. Thus, the blowing-induced nose-bluntness effect in Fig. 3 could have eliminated or greatly reduced the microasymmetry effect on the starboard half of the forebody, permitting the inherent, unimpaired microasymmetry effect on the opposite side to dominate and flip the side force in the opposite direction when $C_{\dot{m}} \to 0.00020$. The nose disturbance in Fig. 6 consisted of "a small hemispherical bump on one side of the nose," which

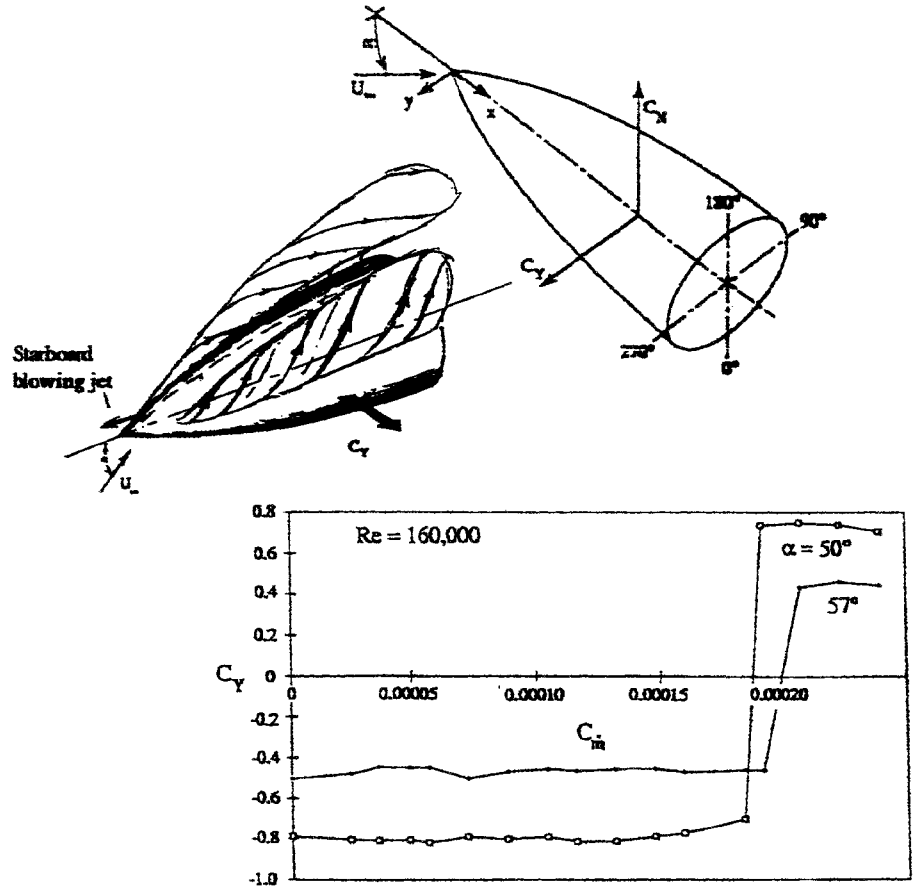

Fig. 3 Effect of nose microblowing on a pointed tangent ogive.[9]

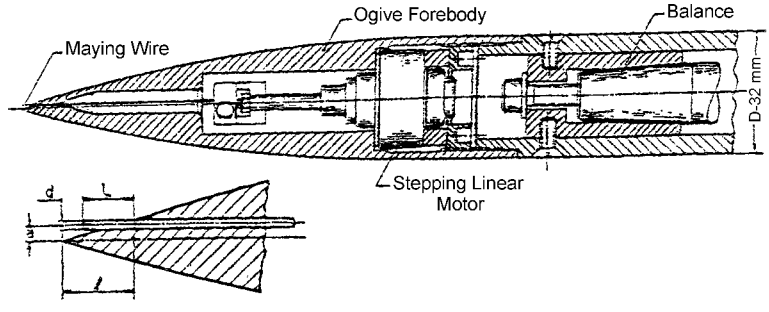

Forebody and disturbance mechanism.

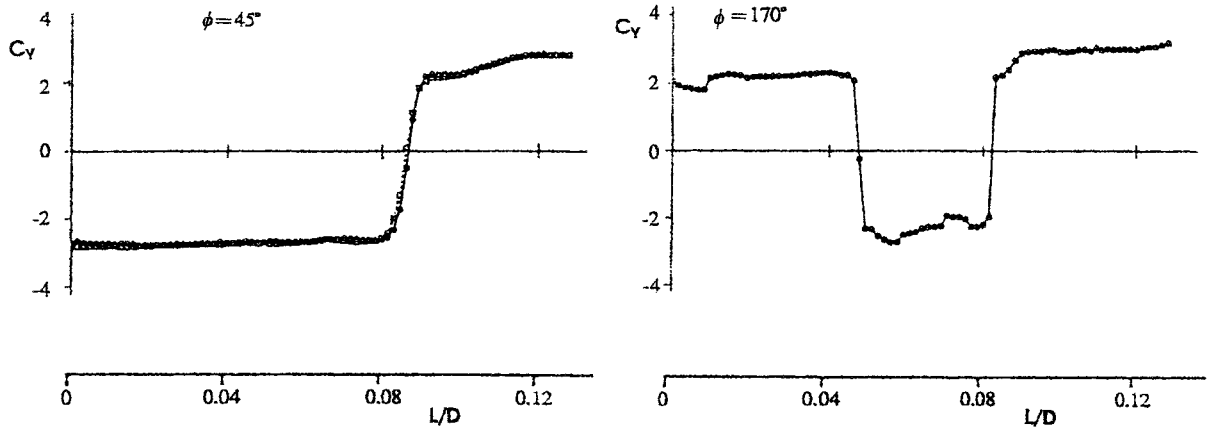

Fig. 4 Effect of wire-rod extension *L/D* at 45- and 170-deg starboard azimuth on measured side force at $\alpha = 40$ deg and $Re = 2.3 \times 10^4$ (Ref. 12).

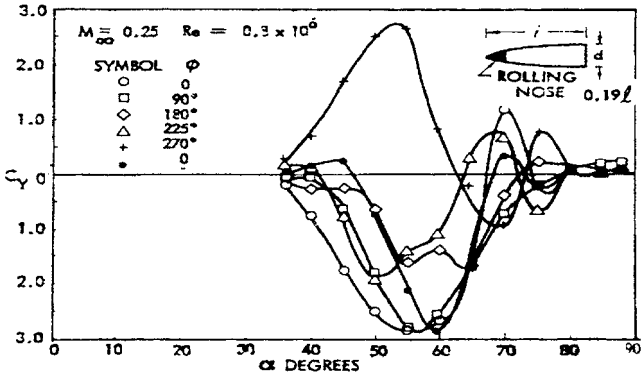

Fig. 5 Effect of nose-tip roll angle on the side force of 3.5-caliber pointed ogive.[13]

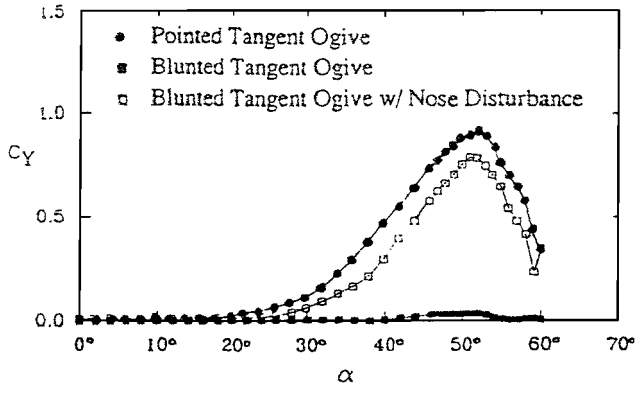

Fig. 6 Effect of 20% nose bluntness on $C_Y(\alpha)$ of 3.5-caliber (pointed) ogive.[14]

caused the blunted tangent-ogive to generate a side force of almost the same magnitude as for the pointed nose, indicating that successful control characteristics could be obtained by nose blowing on the 20% blunt tangent-ogive, in agreement with the results[9,14] shown in Fig. 8. ($C_{\dot{m}} > 0$ designates starboard-side forward blowing.) No explanation is given in Ref. 9 or Ref. 14 for the use in Fig. 3 of the unusual definition of positive C_Y. ΔC_Y is presumably the blowing-induced change of C_Y. As could be expected from Fig. 6, the 20% nose bluntness made the port ($C_{\dot{m}} < 0$)- and starboard-side ($C_{\dot{m}} > 0$) blowing effective at $|C\dot{m}|$ values approaching zero, in stark contrast to the results for the pointed ogive cylinder (Fig. 3), where a change of the starboard blowing rate had no effect until it reached the critical level where it could overpower the port-side microasymmetry effect, reversing the direction of the side force.

The microblowing concept has been applied to a pointed ogive cylinder with 25.4-deg apex half-angle[16,17] (Fig. 9). (For a tangent ogive the included apex angle would be 50.8 deg, not 58.0 deg. Note also the conventional definition of C_Y.) As expected from Figs. 3 and 4, nose blowing on this pointed tangent ogive produced a highly nonlinear, almost discontinuous change of the side force, both in water-tunnel tests,[16] $Re = 0.007 \times 10^6$ at $\alpha/\theta_A = 1.97$ (Fig. 10a), and in wind-tunnel tests,[17] $Re = 0.176 \times 10^6$ at $\alpha/\theta_A = 1.58$, 1.97, and 2.36 (Fig. 10b). The laminar test results in Fig. 10a are according to expectations, as $\alpha/\theta_A \approx 2$ (Ref. 4). However, the results for $Re = 0.176 \times 10^6$ in Fig. 10b raise some questions. Why is the flow separation asymmetric at $\alpha = 40$ deg, where $\alpha/\theta_A = 1.58 < 2$ and the forebody flow separation is expected to be symmetric.[4] Also, why is $|C_Y|$ less at $\alpha = 60$ deg than at $\alpha = 40$ and 50 deg? The only obvious possibility at $\alpha = 40$ deg is that the blowing orifices had generated the separation asymmetry measured at $C_\mu = 0$, possibly through slightly different effects on crossflow boundary-layer transition[6] (Fig. 1), a distinct possibility for the $Re = 1.6 \times 10^5$ test Reynolds number. Blowing orifices have been found to have significant effect on the measured side force of a slightly blunted 5-deg cone[18] (Fig. 11). The figure shows that for upstream blowing, as in

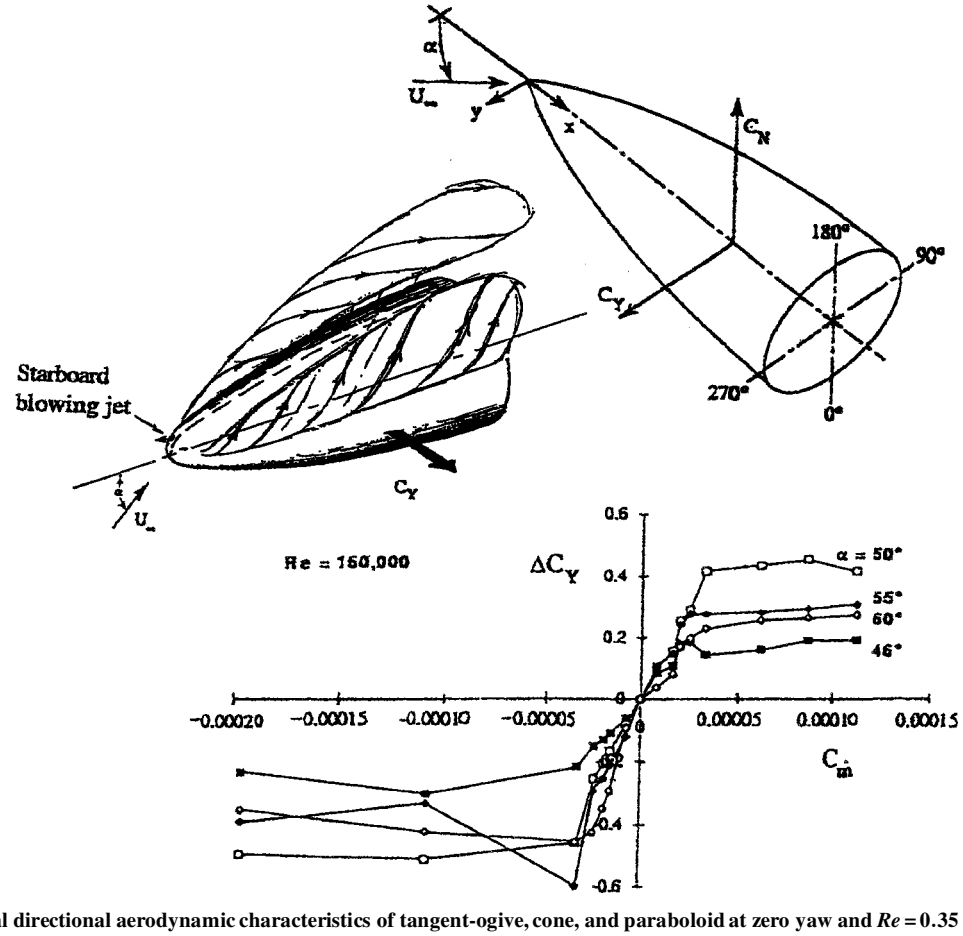

Fig. 7 Lateral directional aerodynamic characteristics of tangent-ogive, cone, and paraboloid at zero yaw and $Re = 0.35 \times 10^6$ (Ref. 15).

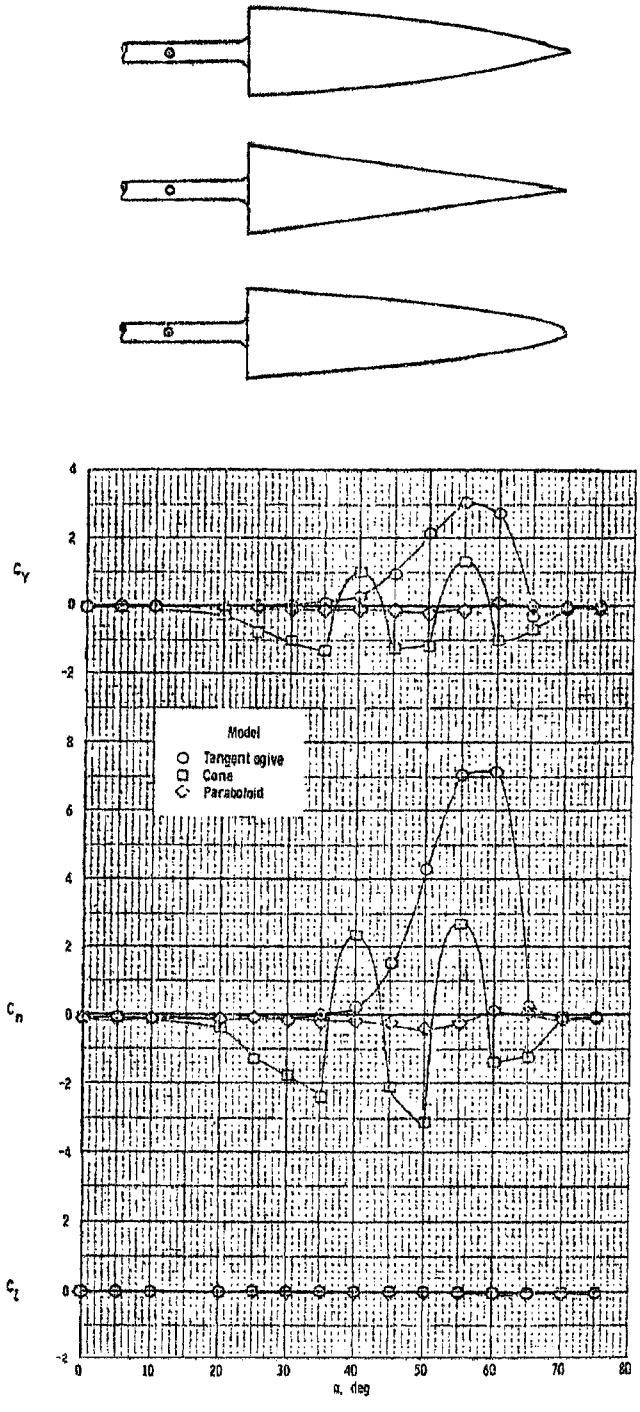

Fig. 8 Side-force control on blunted tangent-ogive.[9]

the case discussed here, the side force measured for $C_\mu = 0$ is of the same magnitude as the largest side force measured for $C_\mu \neq 0$, but of the opposite sign. At $\alpha = 60$ deg (Fig. 10b) Karman vortex shedding occurs on the cylindrical aftbody,[10,11] explaining the decreased $|C_Y|$ value.

To produce the desired linear control characteristics at $\alpha > \theta_A$, a design was proposed that used high-frequency alternating port- and starboard-side blowing in which the time-average dwelling time τ/T at the two asymmetric conditions could be controlled.[17,19] In wind-tunnel tests of the pointed ogive cylinder (Fig. 9), this dynamic blowing technique produced the desired linear control characteristics[17] (Fig. 12), although the slope $\partial C_n/\partial(\tau/T)$ was

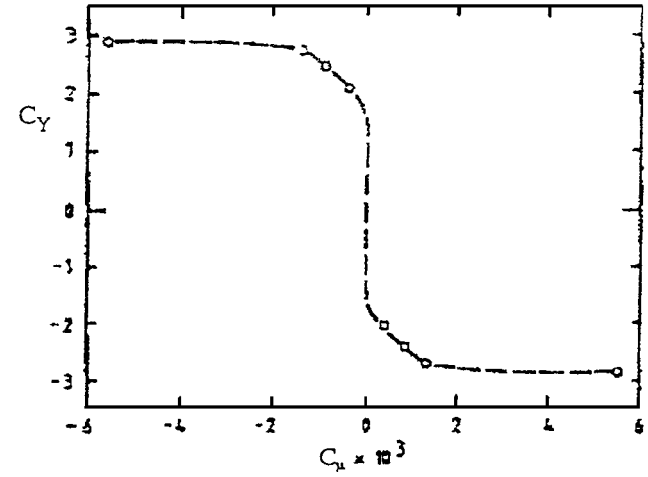

a) At $\alpha = 50$ deg and $Re = 7 \times 10^3$ (Ref. 16)

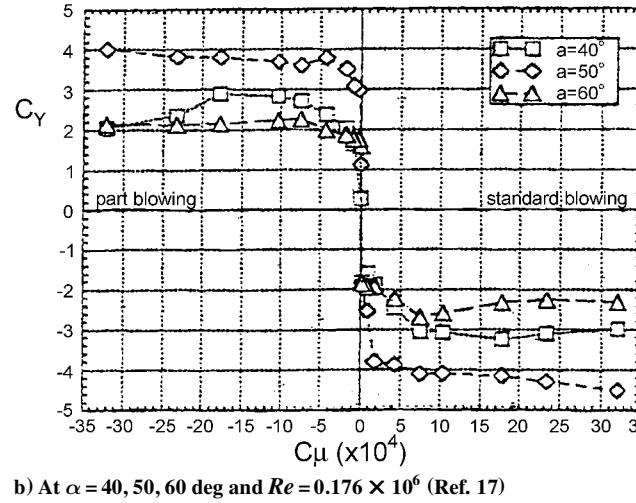

b) At $\alpha = 40, 50, 60$ deg and $Re = 0.176 \times 10^6$ (Ref. 17)

Fig. 10 Effect of jet blowing momentum on side force of pointed ogive cylinder.

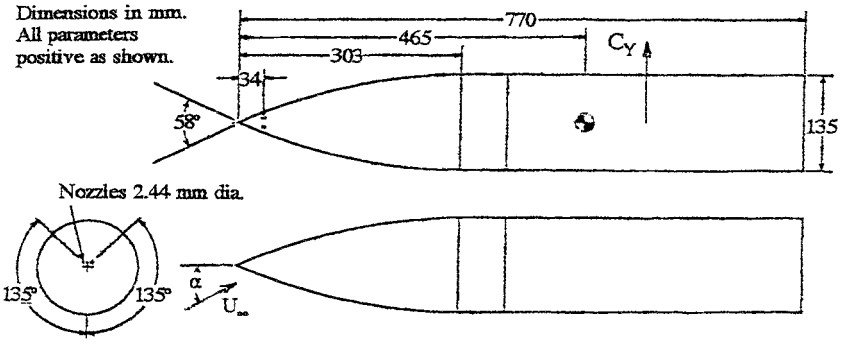

Fig. 9 Pointed ogive-cylinder model used in water-tunnel and wind-tunnel tests.[16,17]

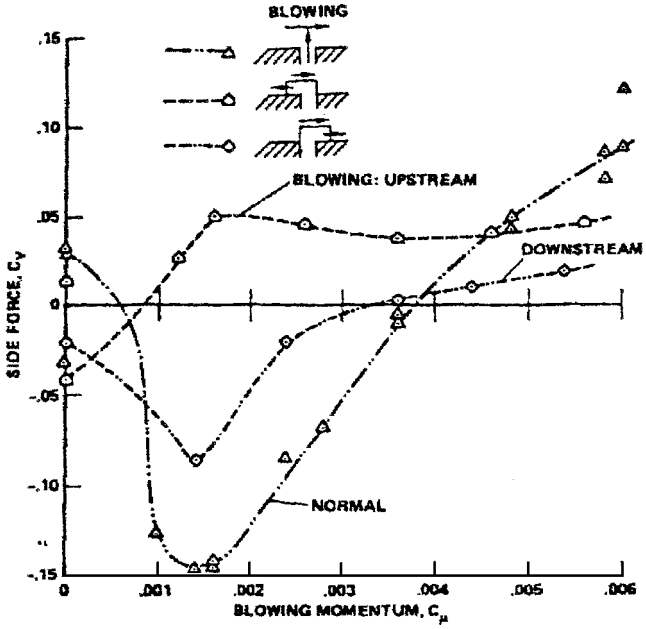

Fig. 11 Effect of blowing method on starboard blowing effect on a 5-deg pointed cone.[18]

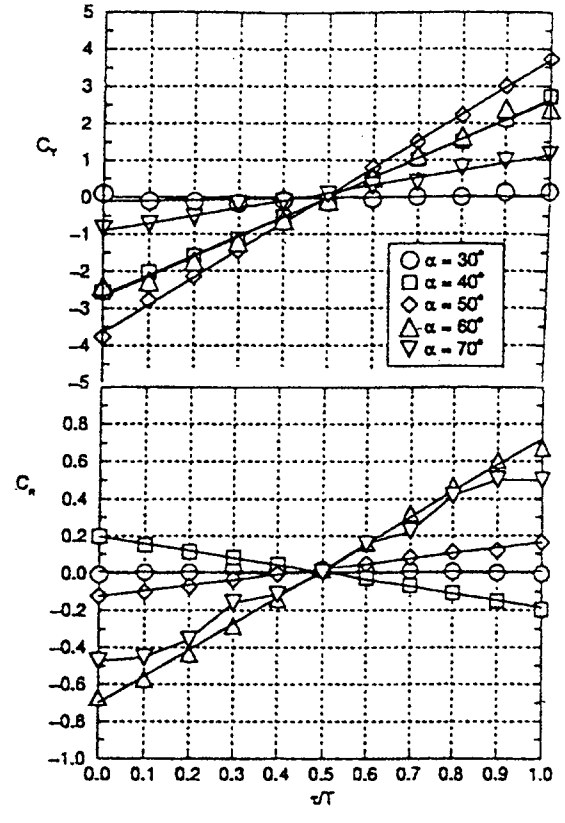

Fig. 12 Effect of duty-cycle τ/T on the side force and yawing moment of a pointed ogive-cylinder body.[16]

negative for $\alpha = 40$ deg ($\alpha/\theta_A = 1.33$) and positive for $\alpha \geq 50$ deg ($\alpha/\theta_A \geq 1.67$), typically the result of a multicellular side-force distribution.[4] As will be discussed later, this undesirable characteristic can be eliminated by using geometric nose bluntness.

When trying this blowing technique on a 65-deg delta-wing-body model with a pointed, slender nose, $\theta_A = 12.8$ deg (Fig. 13), wind-tunnel tests[19] at $\alpha = 45$ deg ($\alpha/\theta_A = 3.5$) gave the results shown in Fig. 14. Only by increasing the blowing beyond $|C_\mu| = 0.0020$ could useful characteristics be obtained (Fig. 15), similar to those in the water-tunnel tests[16] (Fig. 12). Comparing the $\phi = 135$ deg orifice location in Fig. 13 with the $\phi = 170$ deg azimuth of the wire-rod mechanism in Fig. 4, one would expect the result of the blowing in Fig. 14 to be similar to that for the rod perturbation in Fig. 4. Apparently, a sufficient amount of starboard blowing ($C_\mu > 0$) caused the separation asymmetry to switch direction, the effect being similar to that generated when the rod tip was extended halfway to the tip (Fig. 4). Increasing the blowing to $C_\mu > 0.0020$ in Fig. 14 could have caused the blowing to have a bluntness effect on the starboard side of the nose tip similar to the effect observed in Fig. 4 when the rod was extended to the nose tip, in both cases causing the separation asymmetry to switch direction. Thus, one would expect that simultaneous forward blowing on both sides near the nose tip could be used to neutralize existing microasymmetries to produce zero side force, or, more importantly, zero yawing moment at $\alpha > 2\theta_A$. Results obtained on the Boeing 1804 SST configuration[20–22] demonstrated that a very low level of symmetric blowing ($C_\mu = 0.0003$) was needed to delay the appearance of nonzero C_Y and C_n to $\alpha > 3\theta_A$. Thus, differential blowing should be able to provide proportional control beyond $\alpha = 2\theta_A$.

Flow Physics of Forebody Flow Control

In Fig. 10b, where $\alpha/\theta_A < 2$ for $\alpha = 40$ deg, symmetric flow separation usually persists on a clean forebody, and asymmetric blowing is needed to produce asymmetric crossflow separation with associated nonzero side force. The effect of blowing on the ogive-cylinder model (Fig. 9) at $\alpha = 50$ deg ($\alpha/\theta_A = 1.99$) and laminar flow conditions (Fig. 10a) is of the type illustrated by the experimental results in Fig. 16 for a 5-caliber tangent-ogive model.[15] Forward blowing on a moderately blunt nose tip promotes crossflow separation on the side it is applied, generating a side force through the separation-induced pressure rise and causing the associated forebody vortex to be lifted up from the body surface. This in turn permits the vortex on the opposite, nonblowing side to move inboard under the lifted vortex, generating an increase of the normal force in the manner illustrated in Fig. 16. The flow sketches in Fig. 16 apply to both laminar and turbulent crossflow separation. The results show that when the asymmetric crossflow separation occurs, generating a large side force at $\alpha > 30$ deg, the associated asymmetric vortex configuration produces a substantial increase of the normal force, explaining why Bernhardt and Williams[5] found that the desired lateral response to a control input was often associated with an undesired response in the pitch plane.

The initial conditions at $|C_\mu| = 0$ in Fig. 14 are set by the microasymmetry effect of the blowing orifices, generating the measured nonzero side force. (See earlier discussion of Fig. 11.) The microasymmetry potential is limited to the region immediately aft of the pointed nose, where the boundary layer starts to develop. A comment made by Mark Morkovin in a technical discussion at the AIAA Fifth Annual Structures and Materials Conference, Palm Springs, California, April 1–3, 1964, eloquently describes how the microasymmetry can have such a powerful effect: "What happens at the birth of the boundary layer affects its whole downstream life." Nose bluntness removes the surface area near the apex that is most productive in generating microasymmetry effects, as was demonstrated by the results[14] in Fig. 6. This facilitated obtaining the linear control branches for $|C\dot{m}| < 0.00005$ in Fig. 7.

From an operational standpoint it is, of course, safer to operate with $|C_\mu| > 0.0025$ than with $|C_\mu| < 0.0020$ (Fig. 14). In both cases, for $|C_\mu| > 0.0025$ as well as for $|C_\mu| < 0.0020$, the asymmetry generated by the pulsating jet[16,17] would persist for a finite time Δt after the end of the pulse, as a result of the flow relaxation process. The size of Δt will affect the loading produced by the change of crossflow separation asymmetry and associated vortex formation. Consequently, the effect created in this manner by the blowing method is unsteady, particularly at high blowing strengths $|C_\mu| > 0.0020$, resulting in fluctuations in the loading that vary with the distance from the nose tip. Thus, it should not be surprising that time-averaged C_Y and C_n data might be erratic. The duration of the viscous fairing effect and, therefore, the data scatter would be expected to diminish as τ/T approaches 0 or 1, where the residence time on the unblown side is the smallest. The response time

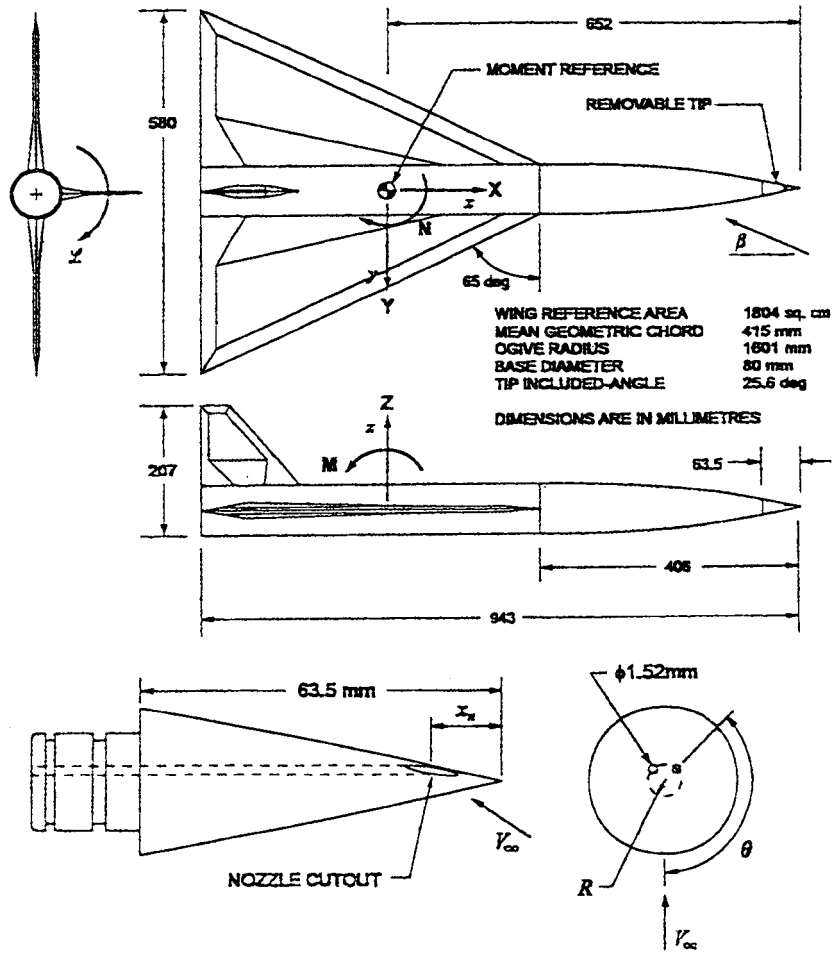

Fig. 13 Tested model of a 65-deg delta wing with a pointed ogive-cylinder body.[19]

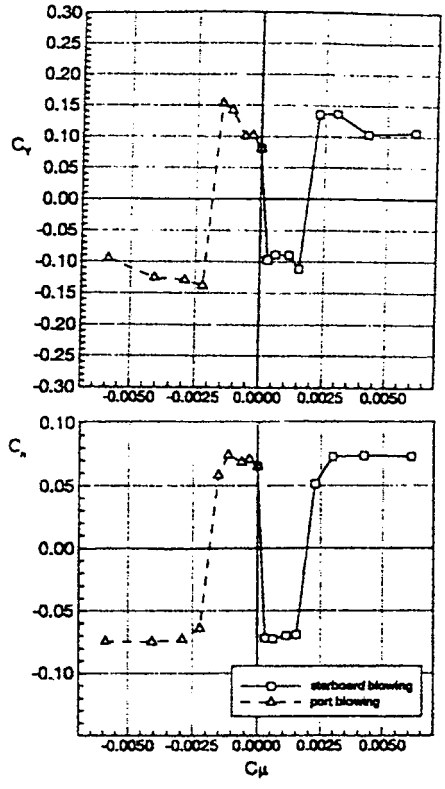

Fig. 14 Effect of jet blowing momentum at $\alpha/\theta_A = 3.5$ and $Re = 0.196 \times 10^6$ on side force and yawing moment of 65-deg delta-wing-body configuration.[19]

to the turning off of the blowing, measured on the full-scale F/A-18, was $1.6 \leq \Delta t/t_c \leq 3$, where t_c is the convection time at freestream velocity.[23] This persistence of unsteady viscous fairing effects on the unblown side might have contributed to the nonlinear $C_Y(\tau/T)$ characteristics in Fig. 15. In contrast, C_n is dominated by the local loading closer to the nose tip, which is relatively insensitive to convective flow time-lag effects, explaining why the $C_n(\tau/T)$ characteristics in Fig. 15 are roughly linear.

It is well established[4] that, in the range $1 < \alpha/\theta_A < 2$, where crossflow separation is symmetric, various types of flow control can change the flow separation to the asymmetric type, the easier the closer the angle of attack is to the included apex angle $2\theta_A$. At $\alpha > 2\theta_A$ the crossflow separation becomes asymmetric and is more difficult to control. This data trend is clearly visible in Fig. 12. At $\alpha = 30$ deg $> \theta_A = 24.9$ deg, the pulsed blowing has no significant effect. At $\alpha = 50$ deg (that is, when α approaches $2\theta_A = 50.8$ deg), the control efficiency reaches its maximum for the side force, but not for the yawing moment. That the yawing moment response changes its direction when the angle of attack is increased from 40 to 50 deg, while the change of side force is insignificant, indicates that the side-force distribution has become multicellular.[4] The dependence of the side-force distribution on α/θ_A has been documented by Hall,[24] using experimental results[25] obtained for a 3.5-caliber tangent-ogive cylinder at $Re = 0.20 \times 10^6$ (Fig. 17). The characteristics $C_n(\tau/T)$ in Fig. 12 demonstrate that a multicellular side-force distribution should be avoided, requiring $t^* < 12$ according to Fig. 17. For the geometry in Fig. 9, where $\xi_{\max} < 6$, one finds that this requires $\alpha < 45$ deg, which is in agreement with the experimental correlation between the $C_Y(\tau/T)$ and $C_n(\tau/T)$ results in Fig. 12.

In addition to being affected by nose blowing, the crossflow separation on a slender forebody is also very sensitive to the Reynolds number[26] (Fig. 18). Increasing the subcritical Reynolds number

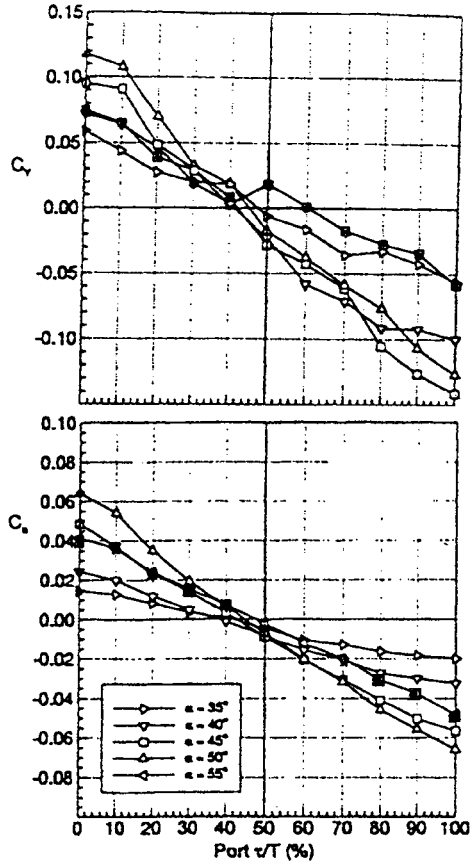

Fig. 15 Effect of duty cycle τ/T on C_Y and C_n of 65-deg delta-wing-body configuration.[19]

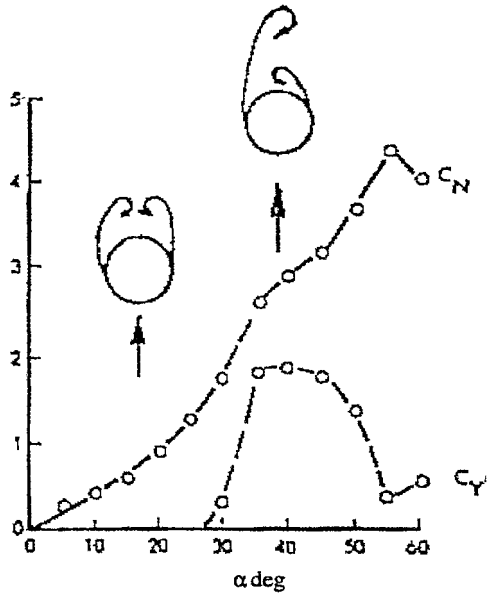

Fig. 16 Measured side force and normal force on a 5-caliber tangent-ogive body.[15]

from 0.28 to 0.44×10^6 more than doubled the magnitude of the side force C_Y and increased $|C_Y|/C_N$ from 0.24 to 1.14, whereas increasing Reynolds number into the critical range ($Re = 0.54 \times 10^6$) almost completely eliminated the side force. Increasing the Reynolds number into the supercritical range ($Re \times 10^{-6} = 0.90$ and 2.03) brought back a side force of significant magnitude. Of course, the yawing moment generated by the side-force distribution depends strongly on the location of the center of gravity of the flight vehicle or in the case of tunnel tests the moment reference axis, as can be

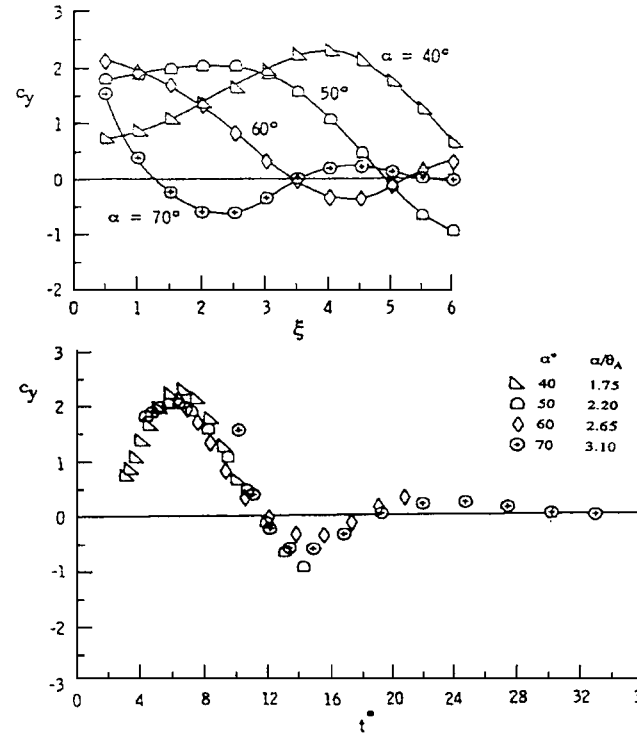

Fig. 17 Local side-force distribution for $l_N/d = 3.5$ tangent-ogive cylinder at $Re = 0.2 \times 10^6$ (Ref. 24).

appreciated from Fig. 18. When considering that the side-force distribution depends on the location and strength of the applied nose blowing, one can appreciate that successful design of forebody flow control is no simple task. Figure 18 supports the statement made in Ref. 27: "For aircraft with clean, axisymmetric forebodies with and without LEXs, conventional rotary tests performed at laminar flow conditions can provide the qualitative full-scale free-flight characteristics." The futility in trying to simulate full-scale flow conditions by the use of tripping devices is conclusively demonstrated in Refs. 27 and 28.

As discussed in Ref. 4, both maximum and minimum $|c_y|_{\max}/c_n$ can occur in the critical Reynolds-number range. At subcritical crossflow Reynolds numbers, asymmetric flow separation occurs near the 90-deg meridian to produce a normalized side force $|c_y|_{\max}/c_n$ of respectable magnitude. As the critical Reynolds-number range is entered, critical/subcritical crossflow separation can take place. This provides the maximum differential in the separation locations on opposite sides of the body, the 80-deg meridian on one side, and the 140-deg meridian on the opposite side, and also provides the maximum suction-pressure differential in the vicinity of the lateral meridian, producing a side force of maximum magnitude. This is illustrated by the results for $Re = 0.44 \times 10^6$ in Fig. 18. The peak is sharp because a relatively small increase of the Reynolds number to $Re = 0.54 \times 10^6$ (or a change of of C_μ or $C_{\dot{m}}$) results in asymmetric, critical flow separation, with nearly equal suction pressures at the lateral meridians. As, in addition, the separation asymmetry in this case is centered around the 140-deg meridian, it is rather ineffective in generating a side force.[26] Thus, both the normalized value $|c_y|_{\max}/|c_n|$ and the side force itself will be very small. Finally, as Reynolds number is increased to the supercritical region ($Re \geq 0.90 \times 10^6$ in Fig. 18), the flow separation asymmetry moves forward toward the 100-deg meridian, where it is once again efficient in generating a side force. This progressive change of the flow separation type from subcritical/subcritical through critical/subcritical and critical/critical to supercritical/supercritical has been observed on a two-dimensional circular cylinder.[29]

Successful design of means for control of forebody flow asymmetry would be simplified greatly if the multicellular side-force distribution, which changes with α/θ_A and the crossflow Reynolds number, could be avoided. As the results[24] in Fig. 17 illustrate, this could

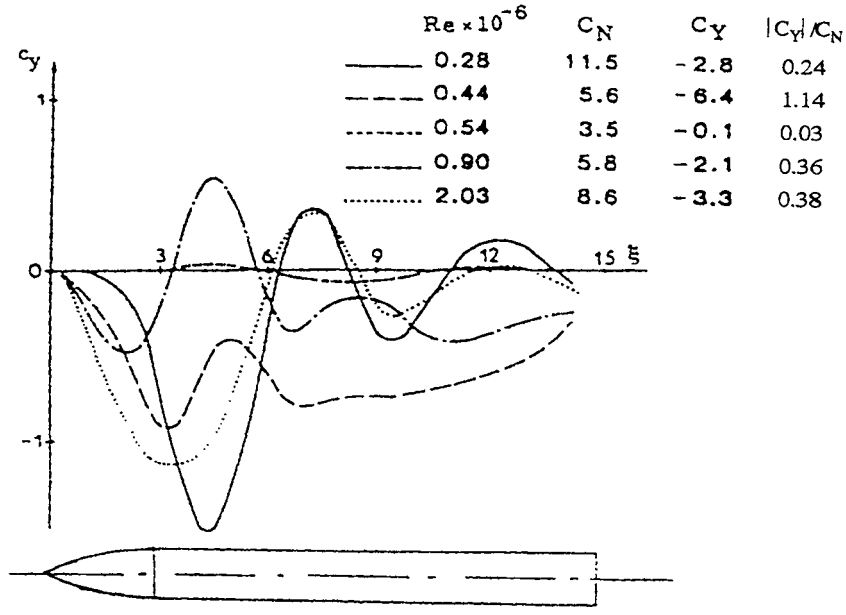

Fig. 18 Side-force distribution at $\alpha = 50$ deg on an ogive-cylinder body through the critical Reynolds-number range.[26]

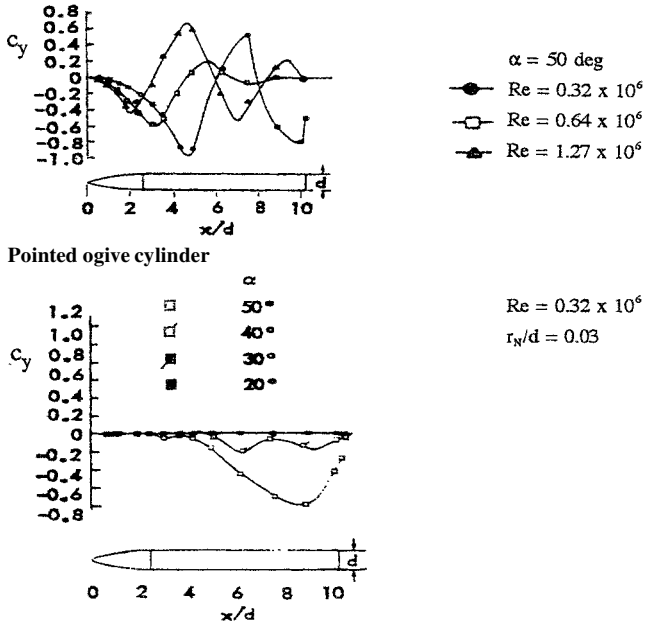

Fig. 19 Side-force distribution at $M = 0.4$ on pointed and blunted ogive-cylinder bodies.[30]

be accomplished by increasing θ_A. This might, however, not be attractive to the vehicle designer when a slender forebody is required, as in the case of the model tested in the wind tunnel[19] (Fig. 13). A more desirable solution would be to use a slight nose bluntness, as is demonstrated by the laminar results[30] in Fig. 19. When considering the method of nose blowing used (Figs. 3, 9, and 13), the applied blowing is likely to generate a viscous nose-bluntness effect, which could be large for a pointed forebody. That this could play a role in producing the control characteristics measured in subscale tests is indicated by the influence of Reynolds number on the nose-bluntness effect generated by the wire-rod apparatus used in Ref. 12. One must, therefore, consider the strong call for caution transmitted by the results in Fig. 18, which demonstrate that "viscous fairing" effects[31,32] are significant on a pointed nose, effects that will be distorted if boundary-layer tripping devices are used.[27] Successful control of forebody crossflow separation and associated vortex shedding requires careful consideration of the lessons learned in the past about asymmetric flow separation on slender bodies of revolution.

Conclusions

Recent investigations of forebody flow control at incidences above the included apex angle have revealed that successful design depends heavily on understanding fully how the fluid mechanics are influenced by the crossflow Reynolds number on the slender forebody, the forebody fineness ratio, the nose bluntness, and finally the geometric locations of the nozzles used for blowing or suction. For the forebody flow control to be viable, the application has to remain within specific ranges of these parameters. The reviewed database suggests that some degree of geometric nose bluntness could greatly simplify obtaining proportional control by using blowing or suction without resorting to any type of the high-frequency switching schemes needed for pointed forebodies.

References

[1]Malcolm, G., "Forebody Vortex Control—A Progress Report," AIAA Paper 93-3540, Aug. 1993.

[2]Grafton, S. B., Chambers, J. R., and Coe, P. L., Jr., "Wind-Tunnel Free-Flight Investigation of a Model of a Spin Resistant Fighter Configuration," NASA TN D-7716, June 1974.

[3]Ericsson, L. E., "Control of Forebody Flow Asymmetry, a Critical Review," AIAA Paper 90-2833, Aug. 1990.

[4]Ericsson, L. E., and Reding, J. P., "Asymmetric Flow Separation and Vortex Shedding on Bodies of Revolution," *Tactical Missile Aerodynamics, General Topics*, edited by M. J. Hemsch, Vol. 141, Progress in Astronautics and Aeronautics, 1992, Chap. 10, pp. 391–452.

[5]Bernhardt, J. E., and Williams, D. R., "Closed-Loop Control of Forebody Flow Asymmetry," *Journal of Aircraft*, Vol. 37, No. 3, 2000, pp. 491–498.

[6]Keener, E. R., "Flow-Separation Patterns on Forebodies," NASA TM-86016, Jan. 1986.

[7]Wallis, R. A., "Boundary Layer Transition at the Leading Edge of Thin Wings and Its Effect on General Nose Separation," *Advances in Aeronautical Sciences, Proceedings of the Second International Congress of the Aeronautical Sciences*, 1970, pp. 161–184.

[8]Almosnino, D., and Rom, J., "Alleviation of the Side Force and Yawing Moment Acting on a Slender Cone-Cylinder at High Angles of Attack, Using Small Jet Injection at Subsonic and Transonic Speeds," Technion—Israel Inst. of Technology, Dept. of Aeronautical Engineering, TAE No. 380, Haifa, Israel, 1979.

[9]Roos, F. W., "Microblowing for High-Angle-of-Attack Vortex Flow Control on a Fighter Aircraft," AIAA Paper 96-0543, Jan. 1996.

[10]Thomson, K. D., and Morrison, D. F., "The Spacing, Position and Strength of Vortices in the Wake of Slender Cylindrical Bodies at Large Incidence," *Journal of Fluid Mechanics*, Vol. 50, Pt. 4, Dec. 1971, pp. 751–783.

[11]Fiechter, M., "Über Wirbel Systeme an Schlanken Rotationskörpern und Ihren Einfluss auf die Aerodynamischen Beiwerte," Franco-German Research Inst., Rapport-Bericht 10/66, Saint-Louis, Dec. 1966.

[12]Degani, D., and Tobak, M., "Experimental Study of Controlled Tip Disturbance Effect on Flow Asymmetry," *Physics of Fluids A*, Vol. 4, No. 12, 1992, pp. 2825–2832.

[13]Keener, E. R., Chapman, G. T., Cohen, L., and Taleghani, J., "Side Forces on a Tangent-Ogive Forebody with a Fineness Ratio of 3.5 at High Angles of Attack and Mach Numbers from 0.1 to 0.7," NASA TMX-3437, Feb. 1977.

[14]Roos, F. W., and Magness, C. L., "Bluntness and Blowing for Asymmetry Control on Slender Forebodies," AIAA Paper 93-3409, Aug. 1993.

[15]Coe, P. L., Jr., Chambers, J. R., and Letko, W., "Asymmetric Lateral-Directional Characteristics of Pointed Bodies of Revolution at High Angles of Attack," NASA TN D-7095, Dec. 1972.

[16]Alexan, K., Hanff, E. S., and Kind, R. J., "Water-Tunnel Investigation of Dynamic Manipulation of Forebody Vortices," AIAA Paper 94-0503, Jan. 1994.

[17]Lee, R., Hanff, E. S., and Kind, R. J., "Linear Control of Side Forces and Yawing Moments Using the Dynamic Manipulation of Forebody Vortices," International Council of the Aeronautical Sciences, Paper 96-2.10.1, Sept. 1996.

[18]Peake, D. J., and Owen, F. K., "Control of Forebody Three-Dimensional Flow Separation," AGARD, CP-262, 1979 (Paper 15).

[19]Lee, R., Hanff, E. S., and Kind, R. J., "The Dynamic Manipulation of Forebody Vortices on a 65 deg Delta-Wing Model," *Proceedings of the 46th Annual Conference*, Canadian Aeronautics and Space Inst., Montreal, Canada, 1989, pp. 251–260.

[20]Takahashi, T. T., Eidson, R. C., and Heineck, J. T., "Aerodynamic Characteristics of a Supersonic Transport with Pneumatic Flow Control," AIAA Paper 97-0043, Jan. 1997.

[21]Beyers, M. E., and Ericsson, L. E., "Considarations in Applying Military Aircraft Forebody Control Methodology to Commercial Aircraft," International Council of the Aeronautical Sciences, Paper 98-3.4.5, Sept. 1998.

[22]Ericsson, L. E., and Beyers, M. E., "Effect of Nose Slenderness on Forebody Flow Control," *Journal of Aircraft*, Vol. 36, No. 5, 1999, pp. 885–889.

[23]Lanser, W. R., and Meyn, L. A., "Forebody Flow Control on a Full-Scale F/A-18 Aircraft," AIAA Paper 92-2674, June 1992.

[24]Hall, R. M., "Forebody and Missile Side Forces and the Time Analogy," AIAA Paper 87-0327, Jan. 1987.

[25]Lamont, P. J., "Pressures Around an Inclined Ogive Cylinder with Laminar, Transitional, or Turbulent Separation," *AIAA Journal*, Vol. 20, No. 11, 1982, pp. 1492–1499.

[26]Champigny, P., "Reynolds Number Effect on the Aerodynamic Characteristics of an Ogive-Cylinder at High Angles of Attack," AIAA Paper 84-2176, Aug. 1984.

[27]Ericsson, L. E., and Beyers, M. E., "Wind-Tunnel Aerodynamics in Rotary Tests of Combat Aircraft Models," *Journal of Aircraft*, Vol. 35, No. 4, 1998, pp. 521–528.

[28]Ericsson, L. E., and Beyers, M. E., "Requirements for Subscale Simulation of Delta-Wing Vortex Characteristics," International Council of the Aeronautical Sciences, Paper 2000-3.10.3, Aug.–Sept. 2000.

[29]Achenbach, E., "Influence of Surface Roughness on the Cross-Flow Around a Circular Cylinder," *Journal of Fluid Mechanics*, Vol. 46, Pt. 2, 1971, pp. 321–335.

[30]Dahlem, V., Flaherty, J., Sherida, D. E., and Przirembel, C. E. G., "High Angle of Attack Missile Aerodynamics at Mach Numbers 0.3 to 1.5," U.S. Air Force Wright Aerodynamics Labs, TR-80-3070, Dayton, OH, Nov. 1980.

[31]Beyers, M. E., and Ericsson, L. E., "Aerodynamic Simulation Difficulties in Subscale Tests of Combat Aircraft," AIAA Paper 99-0683, Jan. 1999.

[32]Ericsson, L. E., "Explanation for Huge Differences Between Measurements of Vortex Breakdown on 65 Deg Delta-Wing Configurations," AIAA Paper 99-4101, Aug. 1999.